Experimental investigation of the thermodynamics of dense plasmas formed from metals at high energy concentrations

B. L. Glushak, A. P. Zharkov, M. V. Zhernokletov, V. Ya. Ternovoĭ, A. S. Filimonov, and V. E. Fortov

Division of the Institute of Chemical Physics, Academy of Sciences of the USSR, Chernogolovka, Moscow Province

An experimental investigation was made of the thermodynamic properties of aluminum, bismuth, and copper at pressures from 0.3 kbar to 14 Mbar and at densities from 10^{-2} to 2.6 of the normal value. A description is given of the apparatus and methods used to create and investigate such states of these metals subjected to shock-wave and adiabatic loading.

I. INTRODUCTION

Interaction of concentrated energy fluxes with matter creates a strongly compressed and heated plasma with pressures in the range of megabars and with a specific concentration of the thermal energy much higher than the cohesive energy of the solid. The medium may enter into complex transient motion accompanied by the creation of powerful shock waves and strongly inhomogeneous dense plasma fluxes. The physical processes can be analyzed and calculations of the parameters of such effects, associated with a high local energy concentration, can be carried out provided reliable information is available on the thermodynamic properties of metals in a wide range of parameters covering all four states of matter.[1-3] In view of the serious difficulties encountered in a theoretical description of strongly compressed and heated media, the required thermodynamic functions are constructed semiempirically[2,3] by collating experimental data obtained as a result of a dynamic interaction with investigated materials.[4,5] The development of semiempirical models for deriving equations of state requires measurements of not only the shock compressibility, but also of the isentropic expansion of shock-compressed (compressed as a result of shock-wave loading) samples[1,4,6] which make it possible to investigate experimentally a range of states of a dense heated metallic liquid and a highly nonideal plasma, which are extremely difficult to describe theoretically.[7]

In the physics of high pressures the most extreme conditions are currently reached by dynamic methods utilizing the technique of shock waves to compress and heat matter irreversibly. It has only recently become possible to carry out investigations at pressures of 2.5 Mbar under static compression conditions,[8] whereas the majority of shock-wave measurements at present are done at pressures $\gtrsim 5$ Mbar using explosive[4,5,9] and pneumatic[10] generators of shock waves. The results of absolute measurements of the shock compressibility of copper and lead at a pressure of about 10 Mbar, reached using explosives, were obtained using apparatus which was not described.[11,12] Methods that make it possible to reach even higher pressures are being studied and developed. They include electrical explosion of foils,[13] the use of powerful laser radiation fluxes,[14] the use of relativistic electron beams,[15] and electrodynamic acceleration of strikers.[16] The use of high explosives has made it possible to increase the record pressure to 4 Gbar (Ref. 17), and the shock compressibility of aluminum has been determined at these pressures.

On the other hand, all the potentialities have not yet been exhausted in the technique of hydrodynamic energy accumulation,[18] based on "gradient" acceleration[18-21] and acceleration of fluxes focused at the center or on a symmetry axis.[22,23] Condensed explosives can be used to create powerful shock waves in suitable systems, providing an opportunity for experimental investigation of the shock compressibility and isentropic expansion of continuous media in the range of pressures inaccessible to conventional explosive methods,[1,5] still sufficiently low to avoid the use of a complex and expensive method of strong explosions.[17,24,25,26] The working range of such high-pressure generators covers also the states on shock adiabats of metals at pressures on the order of several megabars, which are the starting point for the penetration, by isentropic expansion, into the two-phase and near-critical regions of the phase diagram of the investigated matter.[4]

The present paper gives the results of experimental investigations of dense metal plasmas in the megabar range of pressures using shock compression methods and isentropic unloading. Measurements were made on aluminum, copper, and bismuth, metals used widely as construction materials in experimental and technological systems operating subject to strong pulses. Aluminum moreover can act as a reference metal in shock-wave investigations at high and ultrahigh pressures,[28-30] so that its thermodynamic description should be more precise.

Shock waves have been generated by linear explosive launchers,[1,4,5] which employ acceleration of flat metallic strikers by the products of detonation of condensed explosives to velocities $W = 5$–6 km/s. Widening of the investigated part of the phase diagram of the investigated metals can also be achieved employing high-velocity explosive launchers utilizing the phenomenon of irregular reflection of conically converging shock waves[22,23,31] and the principle of energy accumulation in linear layer systems.[18,19] The new data were analyzed together with the results of experiments[32,35] corrected allowing for new detailed measurements of the parameters of launchers and recent data on reference shock adiabats of screens[36] and gaseous barriers.[37] This has made it possible to determine experimentally the points in important parts of phase diagrams of aluminum,

copper, and bismuth at pressures from 14 Mbar to 0.3 kbar and densities from $2.6\rho_0$ to $10^{-2}\rho_0$ (ρ_0 is the normal density), corresponding to strongly compressed and heated degenerate plasma states and a quasi-ideal Boltzmann plasma including high-temperature boiling and condensation curves in the vicinity of the critical point. These results provide the basis for deriving wide-ranging semiempirical equations of state,[2,3] necessary for a physical description of the effects of strong pulses on materials.

2. APPARATUS AND DIAGNOSTICS

The dynamic methods for the investigation of thermophysical properties of matter at high pressures and temperatures are based on the use of the laws of conservation of mass, momentum, and energy in the algebraic (plane steady-state shock wave) or integral (simple rarefaction wave) forms relating thermodynamic and kinematic parameters of the medium.[1,4] We determined thermodynamic properties of metals subjected to shock wave loading, which was done employing the reflection (continuous and porous samples of bismuth) and deceleration (samples of aluminum, bismuth, and some of the copper samples) methods based on the laws governing the decay of an arbitrary discontinuity when the shock waves go from a reference material into an investigated sample or as a result of impact on the investigated target of strikers with known dynamic properties.[1,5]

States of lower (relative to the solid state) density were attained by isentropic expansion of a shock-compressed metal in media with lower values of the dynamic impedance ρC_0 and with known shock adiabats.[3,5,38] Conversion from gas dynamic ($P-U$) to thermodynamic ($P-V-E$) variables involves evaluation of the Riemann integrals describing the laws of conservation for a given type of self-similar flow[1]:

$$V_s = V_a - \int_{P_a}^{P_s} \left(\frac{du}{dP}\right)^2 dP, \quad E_s = E_a + \int_{P_a}^{P_s} \left(\frac{du}{dP}\right) P\, dP, \quad (1)$$

where the index a refers to the initial state on a shock adiabat and the index s represents corresponding states on an isentrope. The parameters of the initial state were determined from the measured values of the wave velocity D and mass velocity U of a shock wave in samples of metals in accordance with the laws of conservation at the front of a plane shock discontinuity[1]: $P_a = \rho_{00}DU$, $V_a = (D-U)/\rho_{00}D$, $E_a = U^2/2 + E_0$, where ρ_{00} is the initial density of a porous sample. The use of barriers of different dynamic rigidity made it possible to study the behavior of the expansion isentropes $P = P_s(U)$ originating from states on shock adiabats when the plasma density increased to several megabars, right up to the gaseous range where pressures were hundreds of bars.

The first series of experiments was carried out on solid and porous bismuth samples. Porous samples were used to increase the effects of irreversible heating as a result of shock-wave compression.[1,6,12,39,40,41] In this series of experiments we detected states of shock compression of a sample with a porosity $m = \rho_0/\rho_{00} = 1.0, 1.48, 1.92, 1.96, 2.45, 2.85$ and we investigated isentropes of unloading from states on adiabats characterized by $m = 1$ and $m = 2.45$. Shock loading was due to planar explosive-driven end launchers[1-5] in which the investigated samples were in contact with alumi-

num, copper, or iron screens. Shock waves were excited in the screens by deceleration of aluminum or steel plates driven by the products of detonation of condensed explosive substances. The intensity of shock waves in the screens of each type of charge was determined in a separate series of experiments.

The wave velocity D in bismuth and the screens was determined by an electric-contact baseline method. Electric-contact sensors were copper wires 0.5 mm in diameter with a fiber thread insulation, which were bonded by an epoxy resin into apertures 0.8 mm in diameter in layers of the target and polished down flush with the lower surface of each layer. Insulation between the layers was ensured by a Mylar film 15 μm thick. The sensors were located on plane surfaces of the target within a circle 20 mm in diameter at points with known coordinates. A reduction of the stray inductance and an improvement in the profile of the signal were ensured by mounting a pulse-shaping electric circuit directly on the shock wave generator, which also made it possible to reduce the number of connecting wires.

Fast-response S9-4A electronic oscilloscopes were used to record the sensor operation signals. A shared sinusoidal calibration signal (100–200 MHz) was applied directly before measurements using a circuit containing the oscilloscopes and sensors. Then, apart from the sensor signals, a record was made of timing marks which were shared by all the devices. The knowledge of where the sensors were located and when they operated (deduced from the oscillograms) relative to the shared timing marks made it possible to monitor the curvature of the shock wave front and to introduce corrections for its skewness.[42] Target films were held in place by screws. A careful control of the film thickness, of the parallel orientation of its surfaces, and of the sensor-connecting circuit made it possible to record, in each oscillogram, signals at six levels (with a resolution down to 1 ns) and to verify simultaneous operation of sensors in a given plane, so that the wave velocities in solid films could be determined to within 1%. When nonporous solid samples were exposed to air (at atmospheric pressure) or argon (at 10 kbar), the error was 2–2.5%. The mass velocity U and the pressure P were found by the reflection method[1,5] from the measured values of D and the known dynamic adiabats of the screens.[36] The dynamic compressibility of bismuth samples of different initial porosities was determined by this method and the results are listed in Table I (lines 1–32). The experimental data on the compressibility of solid bismuth samples (lines 1–6) were the refined results of Ref. 32 and of measurements carried out in collaboration with Bakanova and Trunin. Samples with lower porosities were pellets compacted from a fine powder consisting of grains of 50 μm size. Estimates and experiments[6,40,41] showed that for this particle size the influence on the measured parameters of shock waves on the air included in the pores was slight. The geometry of the samples (with a diameter of 38 mm and height 2–3 mm) was selected in such a way as to exclude the distorting influence of lateral expansion waves and rear unloading waves due to the components of the apparatus.

The points on the upper parts of the expansion isentropes, close to the points representing the initial states, were obtained by unloading the investigated samples into condensed light barriers in the form of Teflon, polyethylene, and polystyrene of different densities ρ_0. The values of the pa-

TABLE I. Shock compressibility of solid and porous metal samples.

No.	Screen material	Parameters of shock wave in screen**	D, km/s	U, km/s	P, Mbar	ρ/ρ₀₀	S ***

Bismuth, $m=1.00$

No.	Screen material	Parameters of shock wave in screen	D, km/s	U, km/s	P, Mbar	ρ/ρ₀₀	S
1	Fe	0.95	3.37	1.03	0.34	1.44	
2	Al	2.82	4.92	2.06	0.99	1.72	
3	Fe	2.29	5.42	2.39	1.27	1.79	
4	Fe	2.82	6.17	2.92	1.77	1.90	
5	Fe	4.25	7.99	4.37	3.42	2.21	
6	Fe	4.58	8.42	4.67	3.85	2.25	
7	Cu	0.84	3.17	0.99	0.31	1.45	
8	Cu	1.28	3.91	1.39	0.55	1.56	
9	Cu	1.75	4.67	1.93	0.88	1.70	
10	Al	2.70	4.77	1.98	0.92	1.71	
11 *	Cu	1.85	4.81	2.03	0.96	1.73	S_1
12	Al	3.29	5.40	2.38	1.26	1.79	
13	Al	3.69	5.82	2.65	1.51	1.83	

Bismuth, $m=1.48$

14	Cu	0.84	2.66	1.19	0.21	1.22	
15	Cu	1.28	3.50	1.71	0.40	1.32	
16	Cu	1.75	4.39	2.24	0.65	1.38	
17	Fe	2.48	5.46	2.99	1.09	1.50	
18	Al	2.70	4.67	2.42	0.75	1.41	
19	Al	3.29	5.27	2.89	1.01	1.53	
20	Al	3.69	5.64	3.24	1.21	1.59	

Bismuth, $m=1.92$

21	Cu	0.84	2.44	1.29	0.16	1.11	
22	Cu	1.28	3.22	1.87	0.31	1.24	
23	Cu	1.75	4.22	2.44	0.53	1.23	
24	Al	2.70	4.64	2.74	0.65	1.27	
25	Al	3.29	5.35	3.26	0.89	1.33	
26	Fe	2.79	5.80	3.63	1.07	1.39	

Bismuth, $m=1.96$

27	Cu	1.75	4.18	2.46	0.51	1.24	
28	Fe	2.48	5.36	3.30	0.88	1.33	

Bismuth, $m=2.45$

29 *	Cu	1.75	4.06	2.60	0.43	1.13	S_7
30 *	Fe	2.48	5.23	3.51	0.73	1.24	S_8

Bismuth, $m=2.85$

31	Cu	1.75	4.00	2.70	0.37	1.08	
32	Fe	2.48	5.19	3.64	0.65	1.17	

Bismuth, $m=1.00$

33 *	Cu	3.35	6.8	3.6	2.40	2.12	S_2
34 *	Cu	3.96	7.6	4.2	3.14	2.24	S_3
35 *	Cu	4.86	8.7	5.0	4.30	2.35	S_4
36 *	Cu	5.55	9.6	5.8	5.4	2.53	S_5
37 *	Cu	6.20	10.6	6.5	6.7	2.59	S_6

Aluminum, $m=1.00$

38 *	Mo	8.30	13.4	5.8	2.1	1.76	S_1
39 *	Mo	9.03	14.0	6.3	2.4	1.83	S_2
40 *	Mo	9.94	14.8	6.9	2.8	1.87	S_3
41 *	Mo	10.43	15.5	7.2	3.0	1.88	S_4
42 *	Mo	12.86	16.9	8.9	4.1	2.12	S_5

Bismuth, $m=1.00$

43 *	Mo	7.00	7.25	3.93	2.8	2.18	
44 *	Mo	7.88	7.8	4.4	3.4	2.29	
45 *	Mo	8.84	8.4	4.9	4.0	2.40	
46 *	Mo	11.35	10.0	6.2	6.1	2.63	

*The initial states on the expansion isentropes of shock-compressed porous samples of bismuth (Table II) and porous samples of aluminum and bismuth (Table III) are identified by an asterisk.

**Lines 1–37 give the mass velocity (km/s) in a screen (reflection method, first and second series of experiments), whereas lines 38–46 give the velocity (km/s) of a striker in the deceleration method (third series of experiments).

***Expansion isentropes in Figs. 3, 5, and 8.

rameters of the expanding metal were determined at different pressure levels by analogy with the determination of the initial states, i.e., using the measured velocities in the barriers. The lower parts of the isentropes were obtained when samples expanded in argon at various initial pressures P_0 from 1 to 30 bar. The velocity of the front of a shock wave in argon was measured bv an optical baseline method employing a fast image-converter camera which recorded the onset of emission of radiation from the plasma as the shock wave emerged from the sample in the gas and the radiation

TABLE II. Unloading isentropes of porous ($m = 2.45$) bismuth samples.

Barrier material*	S_7			S_8		
	D, km/s	U, km/s	P, kbar	D, km/s	U, km/s	P, kbar
Teflon	6.50	2.73	387	7.86	3.59	615
Polyethylene	7.39	3.08	209	8.97	4.14	342
Plastic foam (0.7 g/cm³)	5.87	3.47	143	7.41	4.61	232
Plastic foam (0.5 g/cm³)	5.55	3.70	103	–	–	–
Plastic foam (0.36 g/cm³)	5.36	3.90	75	6.94	5.12	128
Plastic foam (0.3 g/cm³)	–	–	–	6.80	5.18	106
Plastic foam (0.13 g/cm³)	–	–	–	6.78	5.68	48
Argon (30 atm)	–	–	–	7.41	6.35	23.4
Argon (20 atm)	5.86	4.86	9.4	7.53	6.46	16.0
Argon (15 atm)	5.92	4.90	7.2	–	–	–
Argon (10 atm)	6.13	5.12	5.2	8.18	7.09	9.7
Argon (5 atm)	6.39	5.37	2.8	8.33	7.23	5.0
Argon (3 atm)	6.72	5.80	1.9	–	–	–
Argon (1 atm)	7.20	6.26	0.74	9.54	8.53	1.35

*The values in parentheses give the initial density of the barrier material in the case of plastic foam and the initial gas pressure in the case of argon.

showed a strong enhancement when the front of the wave reached a Plexiglas barrier located at a given distance from the target.[11,43]

The results of measurements of the wave velocities in condensed and gaseous barriers during unloading of shock-compressed porous bismuth samples are presented in Table II, where each experimental point corresponded to a value averaged between two and six experiments. The material velocities U and the pressures P in the barriers were calculated using linear DU relationships with coefficients from Ref. 6. The values found in this way, which were equal (because of the conditions for continuity at a contact edge) to the corresponding characteristics of bismuth in isentropic unloading waves are also included in Table II. The flow parameters during isentropic expansion of shock-compressed continuous samples of bismuth unloaded in aluminum, Plexiglas, argon, and air at atmospheric pressure are listed in Table III.

Higher shock compression parameters were obtained

TABLE III. Isentropic expansion of shock-compressed solid of bismuth and aluminum.

| Initial state*	Barrier material	D, km/s	U, km/s	P, kbar	$W_s - 2U$, km/s
	Bismuth, generation of plane shock waves				
11	aluminum	8.76	2.54	603	–
	Plexiglas	7.27	3.14	269	–
	argon (10 atm)	5.20	4.24	3.6	–
	air (1 atm)	5.13	4.60	0.28	0.54
	Bismuth, generation of conical shock waves				
33	aluminum	11.5	4.6	1140	–
	air	9.83	9.0	1.1	1.75
34	aluminum	12.6	5.4	1740	–
	Plexiglas	11.6	6.5	955	–
	air	12.0	10.9	1.6	2.4
35	aluminum	13.9	6.8	2400	–
	Plexiglas	13.7	8.1	1260	–
	air	14.1	12.8	2.2	2.8
36	air	16.2	14.7	2.9	3.1
37	air	18.2	16.5	3.0	3.5
	Aluminum, layer cumulative systems				
38	air	14.9	13.6	2.6	1.9
39	air	16.5	14.9	3.2	2.3
40	air	18.7	16.9	4.1	3.1
41	air	19.1	17.2	4.3	2.8
42	air	24.3	21.8	6.8	3.8
	Bismuth, layer cumulative systems				
43	air	11.3	10.4	1.5	2.4
44	air	11.9	10.9	1.7	2.0
45	air	13.9	12.7	2.3	2.9
46	air	18.1	16.4	3.8	4.0

*Serial number of the line in Table I.
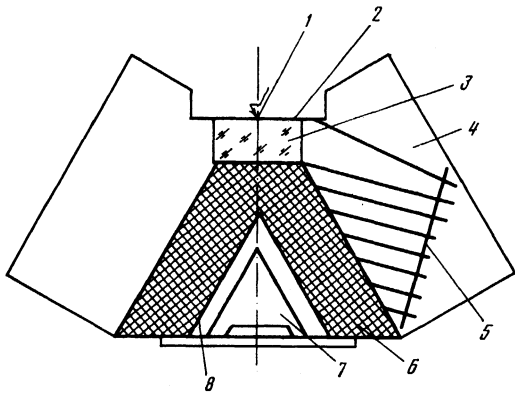
FIG. 1. Generator of conically converging shock waves: 1) explosion initiation point; 2) layer of explosive substance spreading detonation from the initiation point to a circle; 3) inert spacer; 4) generator of a plane detonation wave in the form of an element of a discrete multipoint system for detonation of a conical explosive charge; 5) explosive materials in the channels of a generator of a plane detonation wave; 6) conical charge of an explosive substance; 7) conical sample in which a converging conical shock wave is generated; 8) copper conical liner launched by detonation products produced by the detonation charge 6.

employing conical explosive generators[22,23,31] utilizing the geometric cumulation effect and irregular (Mach) reflection of conically converging shock waves. Additional concentration of energy due to convergence of ultrasonic waves toward the symmetry axis, compared with the planar case,[5] was achieved in this case; moreover the stability of flow was higher than in the spherical case.[41]

The apparatus consisted of a metal cone (which was made of aluminum, steel, or copper) placed inside the cavity of a conical shock-wave generator (Fig. 1). A converging wave was created in a cone either by direct action of the products of detonation or by the shock created in a metal liner (made of aluminum or copper) over the whole lateral surface area of the cone. In the case of a conical shock-wave generator used most frequently in our experiments the velocity of a 3-mm copper liner approaching a cone with a vertex angle 2α amounting to 60° amounted to 2.75 km/sec in the middle part of the lateral surface of the cone. The base distance, in which the linear was accelerated, was 3–4 times greater than its thickness and the convergence of the shock waves along the circular base of the cone was synchronized to better than 50 ns. A Mach wave in a copper cone then had a diameter of 7–8 mm at a distance of 40–50 mm from its vertex, the wave velocity of the Mach disk was 12.1 km/s, and the pressure was $P = 6$ Mbar. A stepped target was placed in a flat-bottomed cylindrical or conical recess of depth at least 10 mm and located at the center of the cone base. The target diameter was 2–2.5 times greater than the diameter of the Mach disk. This configuration made it possible to avoid the influence of unloading waves, traveling along the front of the wave incident from the free surface (cone base), on the parameters of the converging conical shock wave and, consequently, on the parameters of the Mach disk. Measurements were carried out in the central parts of the targets with the diameter of the active region up to 4 mm (in this case the diameter of the Mach high-pressure region was from 6 to 10 mm). This allowed us to analyze the experimental data ignoring the curvature of the Mach disk: we disregarded the streak photographs which recorded a dis-

tortion of the wave pattern because of the curvature of the Mach wave or a random deviation of this wave from the symmetry axis of the cone. The thickness of the target layers (up to 1 mm) and of the diameters of the apertures in them (1–3 mm) were determined from the condition ensuring the absence of the influence of lateral unloading at the edges of the apertures[45] on the assumption that the penetration of shock waves in the material of the sample was weak. A control series of experiments, in which measurements were carried out over baselines from 0.5 to 3.0 mm long, indicated that the attenuation of a Mach wave in the target layers was at most 2–2.5% over baselines of this length.

A better understanding of the flow pattern behind the front of a Mach shock wave and a better experimental configuration were ensured by numerical modeling[46] of the physical processes in generators of conical shock waves, carried out using an equation of state of copper valid in a wide range of conditions.[3,6] The identity of the calculated and experimental data confirmed that the parameters of the target and measurement circuit were selected correctly.

The gasdynamic parameters were determined using an optical baseline method. We measured the radiation which appeared when a shock wave reached the free surfaces of the target. Time-resolved radiation intensity was recorded photographically using Imacon-640 (50–100 ns/mm scale) and Kadr-2 (10–20 ns/mm scale) image-converter cameras. Before each series of experiments the apparatus was calibrated in order to check that the linearity and the actual scale agreed with the nominal one.

An analysis of the experimental data was made by the reflection method in which copper was used as a comparison reference material. Therefore, all the target configurations included a copper substrate. The parameters of shock waves in this substrate were determined in a preliminary series of experiments using generators of conical shock waves and, as far as possible, were monitored in the remaining experiments. At pressures up to 9 Mbar the calculations were carried out using a shock adiabat of copper[36] $D = 3.899 + 1.520U - 0.0071U^2$, whereas at higher pressures use was made of the results of calculations based on the equation of state of Ref. 6, which was in good agreement with the experimental results.[44]

The values of the shock compressibility of solid bismuth samples obtained in the experiments involving irregular reflection of conically converging shock waves are listed in Table I (lines 33–37). The results of experiments on isentropic expansion of shock-compressed bismuth in aluminum, Plexiglas, and air, corresponding to the states on the shock adiabatic in I, are given in Table III. The data on shock compression and isentropic unloading of copper samples as well as the thermodynamic parameters calculated from the equations of state of Ref. 6, demonstrating a spectrum of the pressures realized using conical shock-wave generators described above, as well as the parameters of copper screens used in the bismuth experiments, are all collected in Table IV (lines 2–6). The tabulated values were obtained by averaging the results of measurements of the wave velocities over between four and ten experiments and there were two independent measurements in each experiment; the error of these data was estimated to be 3% and the confidence limit was 0.95.

An alternative method for increasing the launching ve-

743   Sov. Phys. JETP **69** (4), October 1989

Glushak *et al.*   743

TABLE IV. Shock compression isentropic unloading parameters of copper samples (measurements and calculations based on Ref. 6) attainable using shock wave generators available at present.

No.	Type of shock wave generator	Shock loading						Unloading		
		D, km/s	U, km/s	P, Mbar	V, cm³/g	S, J·g⁻¹·K⁻¹	T, к	W_s, km/s	P_s, kbar	S *
1	GPSW	6.68	1.85	1.1	0.081	0.55	2 200	–	–	S_5
2	GCSW	8.9	3.35	2.7	0.070	1.06	5 600	7.2	0.69	
3	GCSW	9.8	3.96	3.5	0.068	1.25	8 000	–	–	
4	GCSW	11.1	4.86	4.8	0.063	1.48	13 200	–	–	
5	GCSW**	12.1	5.55	6.0	0.061	1.63	17 300	12.3	2.04	S_6
6	GCSW**	13.1	6.2	7.3	0.059	1.78	22 400	14.5	2.8	S_7
7	GCSW + LCS	13.9	6.8	8.4	0.057	1.89	27 250	16.0	3.5	S_8
8	GCSW + LCS	15.7	8.1	11.4	0.054	2.09	39 800	20.4	5.8	S_9
9	GCSW + LCS	17.2	9.2	14.1	0.052	2.24	52 500	23.2	7.3	S_{10}
10	LCS***	9.28	3.5	2.9	0.069	1.14	6 500	7.6	0.77	
11	LCS***	10.4	4.2	3.9	0.067	1.36	10 200	9.4	1.2	
12	LCS***	11.0	4.64	4.5	0.065	1.47	12 350	10.6	1.5	
13	LCS***	12.5	5.7	6.3	0.061	1.70	19 300	13.4	2.4	

*The corresponding isentropes are identified in Figs. 6 and 9.
**In the case of isentropes representing additional unloading in Plexiglas the velocity is D_{PMMA} = 14.4 and 15.9 km/s.
***Values of the mass velocity U obtained by the deceleration method.
Note. Here, GPSW denotes generators of plane shock waves, GCSW denotes generators of conical shock waves, and LCS denotes stratified cumulative systems.

locity of the striker, not associated with centripetal or axipetal motion of detonation and shock waves, involves the use of stratified launching systems.[18,19–21,35] The principle of operation of such systems is based on a mechanism analogous to the acceleration of a light body and its elastic collision with a heavy body.[18] The simplest variant of a one-stage layer configuration consists of metal strikers of different thickness and an intermediate layer of matter characterized by a low dynamic rigidity, acting as an elastic spacer. In contrast to the systems in which the acceleration is due to expansion of an intermediate layer at rest (such as electrical explosions of foils[13]), the expansion phase in a layer configuration with an incident heavy striker occurs in a moving coordinate system, which increases further the launching velocity. Compression of an intermediate layer is performed by the transmitted and reflected shock waves and the conditions of inertial confinement of the components of the system.

In the development of explosive multilayer launching systems we have to face a number of problems associated with the specific nature of the process of multistage acceleration. The operation and optimization of a stratified system was analyzed by a gasdynamic calculation of the parameters of the acceleration process using broadly applicable equations of state and also performing entropy thermodynamic calculations of the heating of the launched strikers. They showed that the main contribution to the heating of a striker comes from the first shock wave transmitted by it and the loading conditions approach isentropic, so that we have to use an intermediate layer with a low dynamic rigidity. Then, a single-stage accelerator can ensure a sufficiently high (by a factor of about 1.5) increase in the velocity of the striker. Calculations show that the maximum velocity attainable for a given thickness of the accelerating and accelerated strikers is also reached when the accelerated striker is subjected to a single shock loading. The distance in which it reaches its final velocity is approximately equal to the initial thickness of the intermediate easily compressed layer. Moreover, such

an acceleration regime reduces the possibility of spalling of the accelerated striker and the selection of the minimum thickness of the spacer minimizes the influence on the process of acceleration of the rear rarefaction wave and the acceleration of the shock wave in the material of the inert intermediate layer.

The third series of experiments was carried out using stratified launching systems. In this case we used an ensemble consisting of a steel accelerating striker, 1 mm thick and 60 mm in diameter, moulded into a steel ring 8–10 mm thick, which was driven by the detonation products of a condensed explosive. The velocity of the striker after acceleration over the distance of 30 mm was 5–5.5 km/s and its flat part striking a Plexiglas spacer 1 mm thick was 30–40 mm in diameter. This made it possible to use accelerated molybdenum strikers (0.1–0.2 mm thick), which were 300 mm in diameter, and to measure the velocities in the central part (up to 12 mm in diameter) of the target. The distance to the target in which the latter striker was accelerated amounted to 1.2–1.5 of the thicknesses of the easily compressed spacer.

A stepped target was 0.3–0.5 mm thick and had recesses of the order of 0.15–0.3 mm deep, which served as the measuring baseline; these recesses were on the side of the incident striker and on the outer side, separated by a fixed distance from a transparent Plexiglas window. The target thickness and the measurement baseline were selected, for given materials of the striker and sample (target), so as to ensure homogeneity of the flow and the absence of a distorting influence of the unloading waves generated on the free surface of the striker at the striker–target interface. The target construction made it possible to record information continuously on the whole flow field, to monitor a quasione-dimensional nature and steady-state conditions over the measuring baseline, and essentially doubled the kinematic information. This made it possible to allow for the distorting influence of the curvature of the striker (its radius of curvature resulting from the natural difference between the load-

ing conditions at the center and at the edges was of the order of 10–30 cm) and to introduce suitable corrections in the case when the conditions differed only slightly from the planar flow.

We used launching systems with one or two acceleration stages. In the latter case a steel striker 2.5 mm thick, accelerated in a distance of 38 mm, was used as the accelerating body, while the first intermediate layer was a 5-mm thick spacer made of an explosive. The construction of the main stage was the same for both variants of the experiments.

The range of velocities of molybdenum strikers in one- and two-stage stratified launching systems of the type described above was widened to 7–13 km/sec compared with 5–6 km/sec in the case of the conventional end launching of metal plates.[5,6] The characteristic time intervals which had to be determined in our experiments were $\sim 10^{-8}$ s which was an order of magnitude less than the times needed to record kinematic parameters in typical explosion experiments.[1–6] For this reason when complex systems were employed, determination of the dynamic compressibility and the parameters of isentropic expansion of shock-compressed solid samples of copper, aluminum, and bismuth was carried out using the optical baseline method. Fast-response highly sensitive Agat SF image-converter cameras[47] made it possible to determine the time intervals to within $\approx 2\%$ when the scale on the screen was 2 ns/mm.

We determined the velocity of an incident molybdenum striker W_{Mo}, the velocity of the front of a shock wave in a metal target using different measurement baselines, and the velocity D_W of a shock wave generated in air at atmospheric pressure by a metal plasma expanding in an unloading wave at a velocity U_s. The mass velocity of U of the shock-compressed substance and the pressure P behind the front of the wave were determined by the deceleration method[5] using the known shock adiabat of molybdenum.[36] The velocity of the free surface W_s was calculated using tables[48] and the velocity of the shock wave in air determined experimentally (from the steep increase in the radiation intensity at the moment of arrival of the first air shock wave at the barrier). Streak photographs revealed clearly not only this time but also when the Plexiglas lost its transparency. However, we were unable to link this time directly to the arrival at the barrier of a substance undergoing unloading or to any other phase of the process. This was due to the fact that the Plexiglas lost its transparency at shock compression pressures between 30 and 130 kbar,[49] and the shock waves circulating in the air gap between the expanding substance and the barrier provided such a pressure only after two or three reflections. The circulating shock waves also compressed the gaseous substance (or the substance in the form of a two-phase vapor-liquid mixture) undergoing unloading, which reduced the expansion velocity. Therefore, our method of determining gasdynamic parameters in the case of isentropic unloading in air was in this case best justified from the physical point of view. This method was used also in experiments involving generators of conical shock waves.

The experimentally determined values of the dynamic compressibility of nonporous aluminum and bismuth samples obtained in stratified launching experiments are listed in Table I (lines 38–46). The corresponding data on isentropic expansion in air, which was at atmospheric pressure, are

given in Table III. The data for copper obtained in the series of experiments are in Table IV (lines 10–13). Each experimental point was obtained by averaging the results of between four and six experiments and the kinematic parameters were determined in these experiments to within an error of 3%.

In a fourth series of experiments we increased the parameters of the shock waves using conical shock wave generators to accelerate strikers in a stratified launching system. A Mach shock wave reaching the base of a cone interacted via a condensed explosive spacer, 1.5–2 mm thick, with an accelerating striker which reached a velocity of the order of 16 km/sec after acceleration over a distance of 2 mm. When this velocity was reached, the molybdenum (0.1 mm thick) or tungsten (0.25 mm thick) striker collided with a target where the velocity measurements were carried out in a region 100–500 μm thick and with a diameter if at most 2.5 mm in the central part. The target had a stepped construction: it consisted of three layers of a combined copper substrate and screen 100–200 μm thick, a base layer up to 500 μm thick, and a Plexiglas layer. These experiments showed that when the diameter of the Mach disk was about 8 mm (and for the selected spacer thickness and the distance between the striker and the target) the distortion of the striker during its acceleration did not exceed the limits beyond which we could not carry out shock-wave measurements. Streak photographs of the experiments carried out in this way indicated that the front of the shock wave in the target retained the shape of a flat disk in the field of vision of the image-converter camera (the diameter of this region did not exceed 6 mm).

The parameters of shock waves in copper and the data on the unloading of copper from the various states in air at atmospheric pressure obtained in this series of experiments are listed in Table IV (lines 7–9). In these experiments we determined only the velocity D in shock-compressed copper and the rate of its expansion during unloading. The other parameters were calculated from the equation of state.[3,6] Line 7 in Table IV sums the results of six experiments, whereas lines 8 and 9 give the results of two experiments each. Combination, in one series of experiments, of two methods for increasing the shock pressure made it possible to investigate for the first time isentropic unloading of a solid copper sample from an initial state at a pressure of 14.1 $\pm$ 1 Mbar at a temperature of the order of 5 eV. In the case of copper there was good agreement between the results of our experiments (line 8 in Table IV) carried out using a stratified launching system and a generator of conical ultrasonic waves with the results reported in Ref. 22, where a similar state on the shock adiabat and during unloading in air was obtained as a result of the interaction between Mach shock waves and the sample. This was additional confirmation of the reliability of the thermodynamic information which we obtained using the methods for creation of powerful shock waves described above.

3. DISCUSSION OF EXPERIMENTAL RESULTS

The new experimental data on aluminum are in good agreement (on the low-pressure side) with the results obtained using explosive and pneumiatic generators of shock waves [10,12,43] and on the very high pressure side with the

results of unique measurements of the absolute compressibility[50] and those obtained using the technique of strong explosions.[17,25,26]

The states of a degenerate aluminum plasma achieved in our experiments had parameters in the range where a phase transition was predicted on the basis of earlier experiments.[51] This transition should result from a major modification of the electron structure when the degree of compression was $\rho/\rho_0 \sim 2$, as confirmed by quantum-mechanical calculations carried out in the spherical approximation by the Hartree method.[52] Our results demonstrated no anomalies whatever which could be attributed to redistribution of electrons between the shells during compression. The new data on the compressibility of the aluminum plasma were in reasonable agreement with the calculations carried out employing the quantum-mechanical augmented-plane-wave-model,[53] which (in contrast to the schematic approximation used in Ref. 52) predicted no phase transition. Similar conclusions were drawn also from calculations of the shock compressibility of aluminum[54,55] in the megabar range of pressures carried out using modified Hartree–Fock–Slater models providing a more accurate description of the exchange effects than the approximation employed in Ref. 52.

An analysis of all the experimental data available at present [10,12,17,25,50] and our results made it possible to describe the shock adiabat of aluminum over a wide range of pressures and densities by a smooth curve (Fig. 2) showing no electronic transitions which would affect the plasma compressibility. Aluminum plasma states attained in our experiments were, according to the equation of state,[3] in the range of reduced densities ($\rho/\rho_0 \sim 0.5$) and large increases in temperature near the curve representing high-temperature evaporation and in the vicinity of the critical point of aluminum (Fig. 3).

Figure 4 shows the experimental shock adiabat of normal-density bismuth plotted using $D-U$ coordinates. We can see that on the low-pressure side the new data are in good agreement with the results of earlier investigations.[32,56] The use of generators of conical shock waves and stratified cumulation systems made it possible to raise the limit of maximum attained pressures on the shock adiabat 6.7 Mbar and,

FIG. 3. Pressure–entropy ($P-S$) diagram of aluminum calculated using the equation of state from Refs. 2 and 3. 1) Shock adiabat of aluminum; 2)–5) isotherms representing 5×10^3, 10×10^3, 20×10^3, and 50×10^3 K, respectively; S_1-S_5 are unloading isentropes representing our results. The shaded regions represent two-phase solid–liquid and liquid–vapor states.

together with the data obtained using generators of planar shock waves, to extend greatly the range of investigated states of shock-compressed bismuth. Determination of thermodynamic states crossed consecutively when a metal expands adiabatically after being subjected to preliminary compression and irreversible heating in the front of a powerful shock wave, made it possible to obtain for the first time the thermodynamic properties of a dense nonideal bismuth plasma in a part of the phase diagram inaccessible to other methods. The experimental data on unloading of bismuth in aluminum, Plexiglas (polymethylmethacrylate), and air made it possible to plot, in the $P-U$ plane, the isentropes S_1, S_3, S_4, S_7, and S_8 (Fig. 5) (the isentropes S_2, S_5, and S_6 could be plotted only approximately on the basis of the available experimental data) and then find the thermodynamic $P-V-E$ variables using the expressions in Eq. (1). A calculation carried out using these relationships indicated that the density of an expanding metal changes by almost three orders of magnitude when crossing states from a strongly compressed metal liquid ($\rho = 2.6\rho_0$) to a quasiideal Boltzmann plasma and a metallic vapor ($\rho = 10^{-2}\rho_0$). Isentropic expansion from the states of the shock adiabat reached in our experiments lifts the degeneracy of electrons, drastically alters the
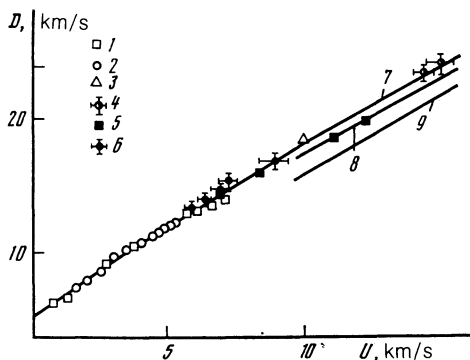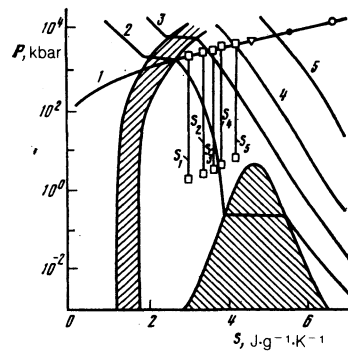

FIG. 2. Velocity ($D-U$) diagram of aluminum. The points are the experimental results taken from 1) Ref. 51; 2) Ref. 53; 3) Ref. 12; 4) Ref. 50; 5) Ref. 58; 6) our results. The curves represent calculations: 7) using the equation of state from Refs. 2 and 3; 8) interpretation of the results of comparative experiments on compressibility of aluminum and quartzite[58]; 9) calculation made on the basis of the Thomas–Fermi model with quantum and exchange corrections.[58]
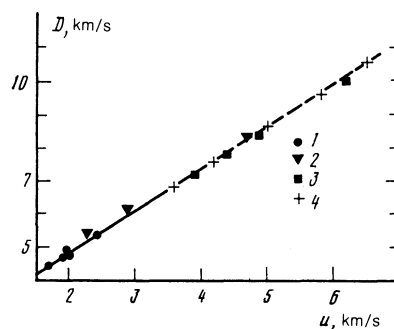

FIG. 4. Shock adiabat of bismuth: 1) results of Ref. 32; 2) experimental results of A.A. Bakanova; 3) results obtained in the present study using layer cumulative systems; results of experiments carried out employing generators of conical shock waves. The continuous curve represents $D = 2.05 + 1.341\ U$ (Ref. 61) and the dashed continuation represents extrapolation to the range of parameters investigated in the present study.
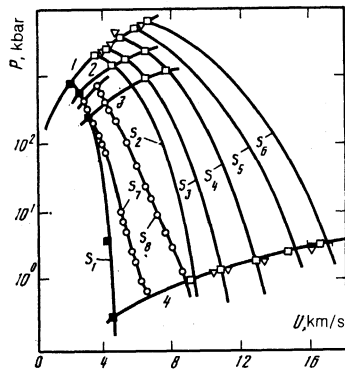
FIG. 5. Shock adiabat and expansion isentropes of bismuth: 1)–4) shock adiabats of bismuth, aluminum, Plexiglas, and air at atmospheric pressure; ■ and ○ (S_1, S_7, and S_8) are the results obtained using linear generators of plane shock waves; ■ (S_2–S_6) are the results obtained employing generators of conical shock waves; ▽ results obtained using layer cumulative systems.

FIG. 7. Deviation from the "doubling" rule exhibited by the velocity of expansion in atmospheric-pressure air of shock-compressed metal samples: 1) results obtained using stratified cumulative systems; 2) results obtained using generators of conical shock waves and of such generators in combination with stratified cumulative systems; 3) results taken from Ref. 60.

electron energy spectrum, induces a metal–insulator transition in the disordered electron structure, and forms a plasma which is nonideal due to various types of the interparticle interaction.

Our experimental results demonstrated that the properties of bismuth change continuously as it expands from the condensed to the gaseous state without significant discontinuities of the thermodynamic functions or any hydrodynamic anomalies which could be interpreted as specific plasma phase transitions.

Figure 6 shows the positions of the experimental points in the P–U plane, the shock adiabats, and the results of calculations[6] of metastable and equilibrium isentropes associated with unloading of copper samples with different initial porosities. The starting points in the calculation of the S_5–S_{10} isentropes were the states on shock adiabats of solid samples
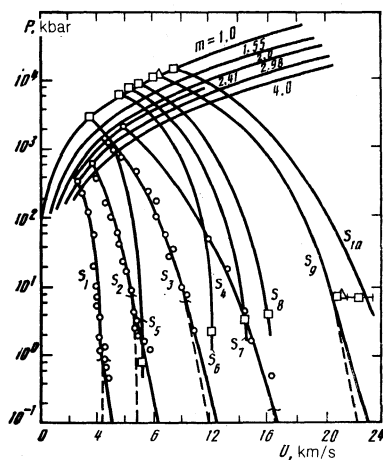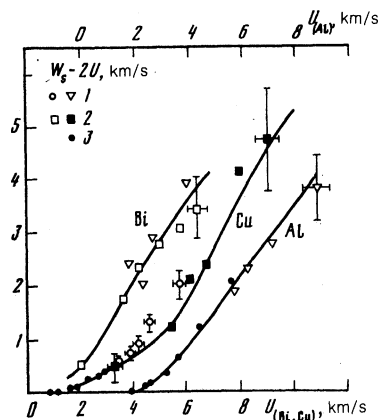
obtained in our experiments. An analysis of the relative positions of the experimental points and calculated unloading isentropes leads to the conclusion that our data are not in conflict with the equation of state of Ref. 6.

Figure 7 shows graphically the experimental values of the quantity $W_s - 2U$, which is a deviation from the "doubling" rule applicable to unloading, as a function of the material velocity U in shock-compressed aluminum, copper, and bismuth samples. The data on aluminum and copper are in satisfactory agreement with the calculated curves reported in Refs. 3 and 6, respectively, whereas the data on bismuth
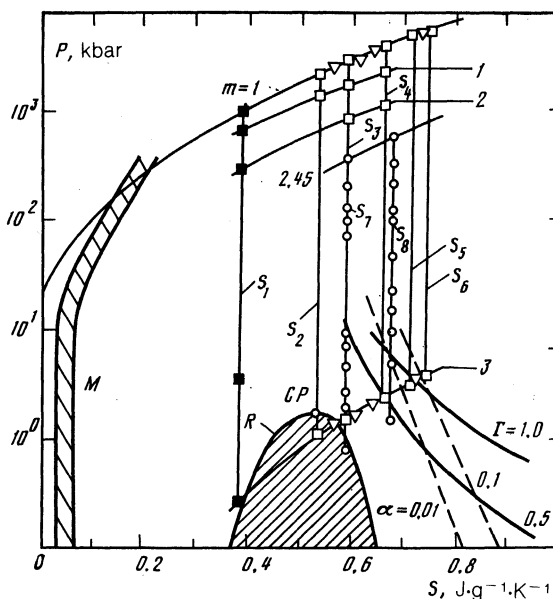

FIG. 6. Shock adiabat and expansion isentropes of copper[6]: m are the shock adiabats for samples with different initial porosities; S_1–S_{10} are expansion isentropes of shock-compressed samples calculated using the equation of state of Ref. 6 with the initial points for the S_5–S_{10} isentropes representing states on the shock adiabat obtained in the present study; the dashed curves are metastable parts of isentropes with the two-phase region; □ represents the results of the present study obtained using generators of conical shock waves (isentropes S_5–S_7) and using generators together with stratified cumulative systems (isentropes S_8–S_{10}); △ represents the results taken from Ref. 22.

FIG. 8. Entropy diagram of bismuth. Here, m are the shock adiabats of nonporous and porous samples; 1–3 are the lines of final states during unloading in aluminum, Plexiglas, and air at atmospheric pressure; M and R are two-phase solid–liquid and liquid–vapor regions; CP is the critical point; Γ represent lines of constant values of the parameter representing deviation from the Coulomb ideal behavior, α are lines representing constant values of the degree of ionization of the plasma. The isentropes S_1–S_8 correspond to Fig. 5.
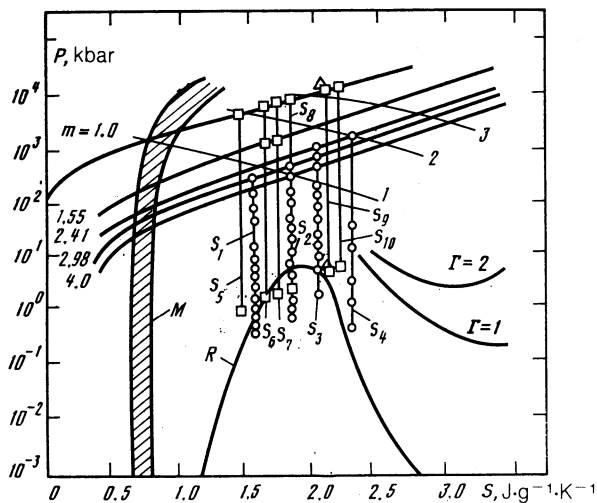
FIG. 9. Entropy diagram of copper.[6] Here, □ are the experimental values obtained in the present study; S_5–S_{10} are unloading isentropes calculated using the equation of state of Ref. 6 for the initial states obtained in the present study; 1–3 are iso-charge lines which are the states reached on shock adiabats of various samples shock-loaded by an iron striker accelerated to velocities of 5, 9, and 15 km/s, respectively.

obtained by two methods are in mutually satisfactory agreement. A considerable deviation from the "doubling" rule provides an independent confirmation of the evaporation of a shock-compressed substance during unloading.[57]

The entropy diagrams of Figs. 8 and 9 show the calculated phase boundaries, which are lines representing constant values of the Coulomb nonideal behavior parameter $\Gamma = (4\pi n)^{1/2}(e^2/kT)^{3/2}$ obtained by plasma calculations by means of the ring approximation in the grand canonical ensemble of statistical mechanics,[37] and lines representing constant values of the degree of ionization $\alpha = n_e/n$ of bismuth. The entropy diagram of bismuth is the result of application of a semiempirical equation of state derived by the method described in Ref. 3 (p. 108). In the case of unloading in air the final states of the isentropes lie in the liquid phase range (here S_1 represents bismuth and S_5 represents copper), in a two-phase vapor–liquid mixture (S_2 and S_7 represent bismuth, whereas S_1–S_3 and S_6–S_8 represent copper), or in a quasiideal Boltzmann gaseous plasma with transcritical parameters (S_3–S_6 and S_8 represent bismuth,whereas S_4, S_9, and S_{10} represent copper). The final state of a supercritical transition in copper from a strongly heated metallic liquid ($P = 14.1$ Mbar, $T = 52\,500$ K, $V = 0.0521$ cm^3/g) to a low-density weakly collisional plasma is characterized by the following calculated parameters: $P = 7.3$ kbar, $T = 9200$ K, $V = 1.3$ cm^3/g, $\alpha = 0.003$. In this region the value of the parameter representing nonideal behavior is close to unity both for copper and bismuth. The degree of ionization of bismuth in this state (lower point of the isentrope S_6) is of order 0.1. A calculation of the equilibrium properties of such a bismuth plasma can be made sufficiently reliably by conventional statistical physics methods and this makes possible the complete thermodynamic description of a substance on the basis of mechanical measurements reported by us, as proposed by Zeldovich.[1,38]

A complete thermodynamic description is achieved because it is possible to calculate the entropy of bismuth in the region of a nonideal gas plasma—lower points of the isentropes S_4–S_6, and S_8—using models of the type described in Ref. 37. According to Refs. 1 and 38, the temperature T of a shock-compressed substance is then found from a thermodynamic identity representing the second law of thermodynamics: $T = (dE + PdV)/dS$, where E, P, and V are known from the measurements of the kinematic characteristics of shock waves for the initial states on the shock adiabat of two adjacent unloading isentropes. There is no need to know the absolute values of the entropy for these isentropes; it is sufficient to find the difference ΔS. Such calculations were carried out in Ref. 59 for copper in the case when the final states of the unloading isentropes lie in the region of the solid phase and it is possible to determine the final temperature of a sample so as to calculate the entropy. Our measurements together with the calculations reported in Ref. 37, make it possible to carry out this procedure for bismuth in the transcritical part of the phase diagram.

[1] Ya. B. Zel'dovich and Yu. P. Raizer, *Physics of Shock Waves and High Temperature Hydrodynamic Phenomena*, 2 Vols., Academic Press, New York (1966, 1967).

[2] A. V. Bushman and V. E. Fortov, Usp. Fiz. Nauk **140**, 177 (1983) [Sov. Phys. Usp. **26**, 465 (1983)].

[3] A. V. Bushman, G. I. Kanel', A. L. Hu, and V. E. Fortov, *Physics and Dynamics of High-Intensity Pulse Interactions* [in Russian], Division of the Institute of Chemical Physics, Academy of Sciences of the USSR, Chernogolovka (1988).

[4] V. E. Fortov, Usp. Fiz. Nauk **138**, 361 (1982) [Sov. Phys. Usp. **25**, 781 (1982)].

[5] L. V. Al'tshuler, Usp. Fiz. Nauk **85**, 197 (1965) [Sov. Phys. Usp. **8**, 52 (1965)].

[6] L. V. Al'tshuler, A. V. Bushman, M. V. Zhernokletov, et al., Zh. Eksp. Teor. Fiz. **78**, 741 (1980) [Sov. Phys. JETP **51**, 373 (1980)].

[7] V. E. Fortov and I. T. Yakubov, *Physics of a Nonideal Plasma* [in Russian], Division of the Institute of Chemical Physics, Academy of Sciences of the USSR, Chernogolovka (1984).

[8] A. Jayaraman, Rev. Sci. Instrum. **57**, 1013 (1986).

[9] *Shock Waves in Condensed Matter* (Proc. Fourth Am. Phys. Soc. Topical Conf., Spokane, WA, 1985, ed. by Y.M. Gupta), Plenum Press, New York (1986).

[10] A. C. Mitchell and W. J. Nellis, J. Appl. Phys. **52**, 3363 (1981).

[11] L. V. Al'tshuler, A. A. Bakanova, and R. F. Trunin, Zh. Eksp. Teor. Fiz. **42**, 91 (1962) [Sov. Phys. JETP **15**, 65 (1962)].

[12] S. B. Kormer, A. I. Funtikov, V. D. Urlin, and A. N. Kolesnikova, Zh. Eksp. Teor. Fiz. **42**, 686 (1962) [Sov. Phys. JETP **15**, 477 (1962)].

[13] K. E. Froeschner, R. S. Lee, H. H. Chau, and R. C. Weingart, in: *Shock Waves in Condensed Matter* (Proc. Am. Phys. Soc. Topical Conf., Santa Fe, NM, 1983, ed. by J. R. Asay, R. A. Graham, and G. K. Straub), North-Holland, Amsterdam (1984), p. 85.

[14] S. I. Anisimov, A. M. Prokhorov, and V. E. Fortov, Usp. Fiz. Nauk **142**, 395 (1984) [Sov. Phys. Usp. **27**, 181 (1984)].

[15] A. F. Akkerman, A. V. Bushman, B. A. Demidov, et al., Zh. Eksp. Teor. Fiz. **91**, 1762 (1986) [Sov. Phys. JETP **64**, 1043 (1986)].

[16] R. S. Hawke and J. K. Scudder, in: *High Pressure Science and Technology* (Proc. Seventh Intern. AIRAPT Conf., Le Crusot, France, 1989, ed. by B. Vodar and Ph. Marteau), Vol. 2, Pergamon Press, Oxford (1980), p. 979.

[17] A. S. Vladimirov, N. P. Voloshin, V. P. Nogin, et al., Pis'ma Zh. Eksp. Teor. Fiz. **39**, 69 (1984) [JETP Lett. **39**, 82 (1984)].

[18] E. I. Zababakhin, *Mechanics in the Soviet Union in the Last Fifty Years* [in Russian], Vol. 2, Izd. AN SSSR, Moscow (1967), p. 313.

[19] V. Ya. Ternovoĭ, *Transient Problems in Hydrodynamics* [in Russian], Institute of Hydrodynamics, Siberian Division of the Academy of Sciences of the USSR, Novosibirsk (1980), p. 141 [Dynamics of Continuous Media, No. 48].

[20]A. G. Ivanov, M. V. Korotchenko, E. Z. Novitskiĭ, et al., Zh. Prikl. Mekh. Tekh. Fiz. No. 2, 86 (1982).

[21]G. R. Fowles, C. Leung, R. Rabie, J. Shaner, in: *High Pressure Science and Technology* (Proc. Sixth AIRAPT Intern. Conf., Boulder, CO, 1977, ed. by K.D. Timmerhaus and M.S. Barber), *Vol. 2, Applications and Mechanical Properties*, Plenum Press, New York (1979), p. 911.

[22]Ph. De Beaumont and L. J. Léygonie, Proc. Fifth Intern. Symposium on Detonation, Pasadena, CA, 1970, p. 430.

[23]O. V. Vazanov, V. E. Bespalov, A. P. Zharkov, et al., Teplofiz. Vys. Temp. **23**, 976 (1985).

[24]L. V. Al'tshuler, B. N. Moiseev, L. V. Popov, et al., Zh. Eksp. Teor. Fiz. **54**, 785 (1968) [Sov. Phys. JETP **27**, 420 (1968)].

[25]E. N. Avrorin, B. K. Vodolaga, N. P. Voloshin, et al., Pis'ma Zh. Eksp. Teor. Fiz. **43**, 241 (1986) [JETP Lett. **43**, 308 (1986)].

[26]C. E. Ragan, Phys. Rev. A **29**, 1391 (1984).

[27]A. A. Leont'ev, V. E. Fortov, Zh. Prikl. Mekh. Tekh. Fiz. No. 3, 162 (1974).

[28]A. C. Mitchell, W. J. Nellis, R. A. Heinle, et al., Physica B (Utrecht) **139–140**, 591 (1986).

[29]A.C. Mitchell, W.J. Nellis, N.C. Holmes, et al., in: *Shock Waves in Condensed Matter* (Proc. Am. Phys. Soc. Topical Conf., Santa Fe, NM 1983, ed. by J.R. Asay, R.A. Graham, and G.K. Straub), North-Holland, Amsterdam (1984), p. 81.

[30]W. J. Nellis, J. A. Moriarty, A. C. Mitchell, et al., Phys. Rev. Lett. **60**, 1414 (1988).

[31]A. P. Zharkov, A. L. Misonochnikov, B. V. Rumyantsev, and V. E. Fortov, "Irregular Reflection of Conically Converging Shock Waves," Preprint [in Russian], Division of Institute of Chemical Physics, Academy of Sciences of the USSR, Chernogolovka (1989).

[32]L. V. Al'tshuler, K. K. Krupnikov, and M. I. Brazhnik, Zh. Eksp. Teor. Fiz. **34**, 886 (1958) [Sov. Phys. JETP **7**, 614 (1958)].

[33]B. L. Glushak, M. V. Zhernokletov, and V. N. Zubarev, Papers presented at First All-Union Symposium on Pulsed Pressures (ed. by S. S. Batsanov) [in Russian], Vol. 1, All-Union Scientific-Research Institute of Physicotechnical and Radio Engineering Measurements, Mendeleevo, Moscow Province (1974), p. 87.

[34]A. V. Bushman, I. K. Krasyuk, P. P. Pashinin, et al., Pis'ma Zh. Eksp. Teor. Fiz. **39**, 341 (1984) [JETP Lett. **39**, 411 (1984)].

[35]A. V. Bushman, B. L. Glushak, V. K. Gryaznov, et al., Pis'ma Zh. Eksp. Teor. Fiz. **44**, 375 (1986) [JETP Lett. **44**, 480 (1986)].

[36]L. V. Al'tshuler, A. A. Bakanova, I. P. Dudoladov, et al., Zh. Prikl. Mekh. Tekh. Fiz. No. 2(126), 3 (1981).

[37]V. K. Gryaznov, M. V. Zhernokletov, V. N. Zubarev, et al., Zh. Eksp. Teor. Fiz. **78**, 573 (1980) [Sov. Phys. JETP **51**, 288 (1980)].

[38]Ya. B. Zel'dovich, Zh. Eksp. Teor. Fiz. **32**, 1577 (1957) [Sov. Phys. JETP **5**, 1287 (1957)].

[39]K. K. Krupnikov, M. I. Brazhnik, and V. P. Krupnikova, Zh. Eksp. Teor. Fiz. **42** 675 (1962) [Sov. Phys. JETP **15**, 470 (1962)].

[40]L. V. Al'tshuler, K. K. Krupnikov, B. N. Ledenev, et al., Zh. Eksp. Teor. Fiz. **34**, 874 (1958) [Sov. Phys. JETP **7**, 606 (1958)].

[41]I.C. Skidmore and E. Morris, Proc. Symposium on Thermodynamics of Nuclear Materials, Vienna, 1962, publ. by International Atomic Energy Agency, Vienna (1962), p. 173.

[42]A. C. Mitchell and W. J. Nellis, Rev. Sci. Inst. **52**, 347 (1981).

[43]L. V. Al'tshuler, S. B. Kormer, A. A. Bakanova, et al., Zh. Eksp. Teor. Fiz. **38**, 790 (1960) [Sov. Phys. JETP **11**, 573 (1960)].

[44]R. F. Trunin, M. A. Podurets, G. V. Simakov, et al., Zh. Eksp. Teor. Fiz. **62**, 1043 (1972) [Sov. Phys. JETP **35**, 550 (1972)]; R. F. Trunin, M. A. Podurets, B. N. Moiseev, et al., Zh. Eksp. Teor. Fiz. **56**, 1172 (1969) [Sov. Phys. JETP **29**, 630 (1969)].

[45]L. V. Al'tshuler, S. B. Kormer, M. I. Brazhnik, et al., Zh. Eksp. Teor. Fiz. **38**, 1061 (1960) [Sov. Phys. JETP **11**, 766 (1960)].

[46]A. V. Bushman, A. P. Zharkov, B. P. Kryukov, et al.,"Numerical modeling of irregular reflection of shock waves in condensed media," Preprint [in Russian], Division of Institute of Chemical Physics, Academy of Sciences of the USSR, Chernogolovka (1989).

[47]B. Z. Gorbenko and B. M. Stepanov, Prib. Tekh. Eksp. No. 4, 185 (1982).

[48]N. M. Kuznetsov, *Thermodynamic Functions and Shock Adiabats of Air at High Temperatures* [in Russian], Mashinostroenie, Moscow (1965).

[49]M. V. Zhernokletov, V. N. Zubarev, and G. S. Teleging, Zh. Prikl. Mekh. Tekh. Fiz. No. 4, 127 (1969).

[50]V. A. Simonenko, N. P. Voloshin, A. S. Vladimirov, et al., Zh. Eksp. Teor. Fiz. **88**, 1452 (1985) [Sov. Phys. JETP **61**, 869 (1985)].

[51]L. V. Al'tshuler and A. A. Bakanova, Usp. Fiz. Nauk **96**, 193 (1968) [Sov. Phys. Usp. **11**, 678 (1969)].

[52]G. M. Gandel'man, Zh. Eksp. Teor. Fiz. **51**, 147 (1966) [Sov. Phys. JETP **24**, 99 (1967)].

[53]A. K. McMahan and M. Ross, in: *High Pressure Science and Technology* (Proc. Sixth AIRAPT Intern. Conf., Boulder, CO, 1977, ed. by K.D. Timmierhaus and M.S. Barber), *Vol. 2, Applications and Mechanical Properties*, Plenum Press, New York (1979), p. 920.

[54]G. V. Sin'ko, Chislennye Metody Mekh. Sploshnoi Sredy No. 12, 121 (1981).

[55]A. F. Nikiforov, V. G. Novikov, and V. B. Uvarov, Dokl. Akad. Nauk SSSR **267**, 615 (1982) [Sov. Phys. Dokl. **27**, 956 (1982)].

[56]R. G. McQueen and S. P. March, J. Appl. Phys. **31**, 1253 (1960).

[57]L. V. Al'tshuler, A. A. Bakanova, A. V. Bushman, et al., Zh. Eksp. Teor. Fiz. **73**, 1866 (1977) [Sov. Phys. JETP **46**, 980 (1977)].

[58]L. V. Al'tshuler, N. N. Kalitkin, L. V. Kuz'mina, et al., Zh. Eksp. Teor. Fiz. **72**, 317 (1977) [Sov. Phys. JETP **45**, 167 (1977)].

[59]V. E. Fortov and A. N. Dremin Fiz. Goreniya Vzryva **9**, 743 (1973).

[60]A. A. Bakanova, I. P. Dudoladov, M. V. Zhernokletov, V. N. Zubarev, and G. V. Simakov, Zh. Prikl. Mekh. Tekh. Fiz. No. 2, 76 (1983).

[61]M. VanThiel, *Compendium of Shock-Wave Data, Vol. 1*, Report No. UCRL-50108, Lawrence Livermore National Laboratory, Livermore, CA (1977).

Translated by A. Tybulewicz